La 5e conférence d'IBPSA - Canada
The 5th IBPSA - Canada Conference
Québec 21-22 mai

COMPUTER MODEL OF THE REFRIGERATION SYSTEM OF AN ICE RINK

Gabriel Teyssedou[1], Radu Zmeureanu[1], Daniel Giguère[2]

[1]Centre for Building Studies, Department of Building, Civil and Environmental Engineering, Concordia University, Québec, Canada

[2]CANMET Energy Technology Centre, Québec, Canada

ABSTRACT

This paper presents the development of a computer model of the refrigeration system of an existing ice rink by using the TRNSYS 16 environment. The ice rink is located in Montréal and the refrigeration system is composed of two chillers using refrigerant R-22. Models have been developed for the chillers, the ice-concrete slab and the controller. The impact of a heat recovery from the condensers on the energy demand for sanitary water heating is estimated. The TEWI criterion is used to estimate the refrigeration system impact on the global warming.

INTRODUCTION

In Canada, indoor ice rinks are an integral part of community life and activities. Ice rinks are used for sports (hockey, free skating, speed skating or figure skating) and on occasion as auditoriums. The ice rinks are often used eighteen hours per day, seven days per week during eleven months each year (ASHRAE 1998).

Studies that examined the energy efficiency of ice rink refrigeration systems are scarce. Gregoire and Zilberberg (1986) used a computer model to analyze the heat flow within the floor of an ice rink. Zmeureanu et al. (2002) simulated the cooling loads of the ice sheet and the energy performance of the refrigeration system using the DOE-2.1E program. Bellache et al. (2005a, 2005b) have investigated the airflow, and heat and humidity transfer in indoor ice rinks, by using a computational fluid dynamics (CFD) model. Daoud and Galanis (2006) have coupled a zonal model to the TRNSYS program to simulate the transient thermal behaviour of an ice rink. The estimated air temperatures above the ice sheet were compared with measurements. Ouzzane et al. (2006) have presented measurements performed in an indoor ice rink located in Montréal. Jung and Krarti (2007) used an experimental set-up to evaluate the impact of four different floor insulations, which are used to prevent heat transfer from the ground, on the refrigeration load of an ice rink.

MONITORED ICE RINK

The ice rink refrigeration system simulated in this study is based on measurements collected in an existing indoor ice rink located in Montréal. The ice surface is 61m long and 26m wide. The refrigeration system is composed of two chillers using refrigerant R-22. Each chiller has three reciprocating compressors driven by 22.4 kW electric motors. Compressors are connected in parallel on the direct expansion evaporator. Each compressor is connected to an air-cooled condenser installed on the roof of the building. The two evaporators are connected in series on the brine side. The brine, a solution of calcium chloride ($CaCl_2$), makes four passes through the concrete slab before returning to the circulating pump. The 12.5 kW pump provides a constant brine mass flow rate. In order to limit the peak power demand, the maximum number of compressors in operation is limited to five. Hence, a compressor in chiller #1 is by-passed and reconnected on the second compressor. The ice is resurfaced at about one-hour interval. The refrigeration system operates 21 hours per day, from 3h00 to 24h00. The schematic of the refrigeration system is illustrated in Figure 1.

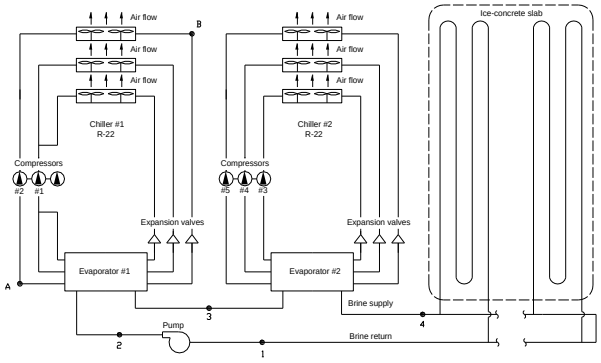

Figure 1: Schematic of the refrigeration system

Camillien-Houde ice rink was equipped with sensors and data loggers to collect information on the operating conditions of its refrigeration system. Measurements were conducted by the CTEC-CANMET-Varennes with

the financial support from an NSERC-Strategic grant and ASHRAE (Ouzzane et al. 2006). Measurements were collected at one-minute intervals during several days of different months by permanently installed sensors. Table 1 presents the long-term measurements used in the current study and the location on the refrigeration system (Figure 1).

Table 1: Measurements of the refrigeration system

Electric demand
Heat flux on the ice sheet
Exterior air temperature
Ice temperature
Return brine temperature (Point 1 in Figure 1)
Brine temperature at the pump exit (Point 2)
Brine temperature at evaporator #1 exit (Point 3)
Brine temperature at evaporator #2 exit (Point 4)
Refrigerant T and P, expansion valve exit (Point A)
Refrigerant T and P, condenser exit (Point B)

The refrigerant and brine mass flow rates have been measured by using a transit-time ultrasonic flow meter, based on the fluid sonic velocity and known pipe dimensions (Scott 2003). They have been evaluated as 0.3348 kg/s (compressor no.1) and 31.324 kg/s, respectively.

MODELS OF THE COMPONENTS

The ice rink refrigeration system was divided into three components: the chillers, the ice-concrete slab and the controller. The mathematical models corresponding to each component have been programmed in C++ and then integrated as an external DLL into TRNSYS.

CHILLERS

The mathematical model of the chiller is based on the ASHRAE Toolkit-I for primary equipment (Bourdouxhe et al. 1997). The Toolkit was developed to evaluate the performance of heating, refrigerating, and air-conditioning equipments (HVAC) by proposing different routines developed in FORTRAN. The models of the ASHRAE Toolkit-I are for steady state regime.

The model of the chiller integrates a direct expansion evaporator, a condenser, and a reciprocating compressor. Each component is modeled in two steps. First, the characteristics of the components are identified based on the analytical model, and the manufacture's catalogue or measured data. Then, the components are simulated for given operating conditions by using the analytical model with the identified parameters.

The reciprocating compressor is modeled as an ideal machine, i.e., irreversibilities are not taken into account. However, the simplified model of the compressor considers the losses due to the "motor-transmission" by analyzing the behaviour of the "motor-transmission" and the behaviour of the reciprocating compressor separately. Figure 2 presents the model of the reciprocating compressor. Electromechanical losses are considered as a sensible heat addition to the refrigerant.

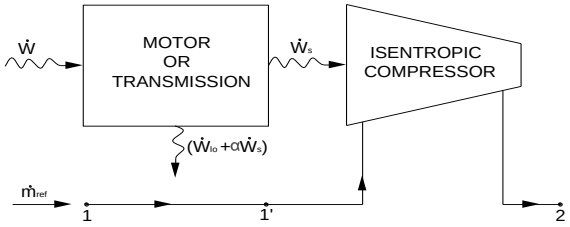

Figure 2: Model of the reciprocating compressor

The power input to the electrical motor is divided in the following components:

$$\dot{W} = \dot{W}_{lo} + \alpha \dot{W}_S + \dot{W}_S \qquad (1)$$

where $\dot{W}$ is the power input to the compressor, $\dot{W}_{lo}$ are the constant electromechanical losses, α the loss factor and $\dot{W}_S$ is the isentropic power of the compressor. Equation 2 relates the behaviour of the reciprocating compressor with the identified parameters:

$$\dot{V} = \dot{V}_s \left[1 + C_f - C_f \left(\frac{P_2}{P_1} \right)^{1/\bar{\gamma}} \right] \qquad (2)$$

where $\dot{V}$ is the volume flow rate of refrigerant, $\dot{V}_s$ is the swept volume flow rate, C_f is the ratio between dead volume and the swept volume, P_2 / P_1 is the compression ratio and $\bar{\gamma}$ is the mean isentropic coefficient.

The Toolkit uses the routine called PISCOMP1, which estimates $\dot{W}_{lo}$, α, $\dot{V}_s$ et C_f (Table 2). A superheating of 6°C at the evaporator and a sub-cooling of 12.5°C at the condenser are considered in the identification of parameters.

Table 2: Compressor identified parameters

Parameter	Value
W_{lo}	6330.472
α	-0.067800
C_f	0.070853
V_s	0.070853

The overall heat transfer coefficients (AU_{evap}, AU_{cond}) are identified as parameters characterizing the heat exchangers by using the collected data and the

routine PISCHIL1. This routine is based on an iterative procedure requiring a wide range of operating points. This routine neglects the sensible heat exchanges in the evaporator and condenser. This approximation could be applicable only to the evaporator since the degree of superheating is very small; however, it is a crude approximation for the condenser since the amount of heat exchanged during de-superheating and sub-cooling is non-negligible.

However, measurements collected at the Camillien-Houde ice rink allow identifying the overall heat transfer coefficients by means of the log mean temperature difference (Equation 3):

$$AU = \frac{\Delta T_m}{Q} \quad (3)$$

where Q is determined by applying the heat balance on the refrigerant side for each heat exchanger, and ΔT_m is the log mean temperature difference (Equation 4):

$$\Delta T_m = \frac{\Delta T_1 - \Delta T_2}{\ln(\Delta T_1 / \Delta T_2)} \quad (4)$$

where ΔT_1 and ΔT_2 are the temperature differences between the two fluids at each end of the heat exchanger. For calculations, the heat exchanger is divided into one part that experiences sensible heat transfer and another part with latent heat transfer. Therefore, two parameters AU are identified for the evaporator, and three parameters AU for the condenser. The calculation of the AU values is conducted for different days of different months to determine the average coefficients. Hence, for the evaporator, the average latent and sensible heat transfer coefficients are $AU_{evap,lat.}$=13,238 W/°C and $AU_{evap,sens}$=337 W/°C, respectively. For the condenser, the average latent coefficient is $AU_{cond,lat.}$=4,862 W/°C, while the sensible coefficients corresponding to de-superheating and sub-cooling are equal to $AU_{cond,sens\text{-}desupheat.}$=1,385 W/°C and $AU_{cond,sens\text{-}subcool}$=423 W/°C, respectively.

By using the four parameters of the compressor, and the latent overall heat transfer coefficients of the evaporator and condenser with the routine PISSIM1, it is possible to perform the simulation of the chiller. This routine consists into a series of iterative loops that determines the electric demand of the compressor, the load at the evaporator and condenser, the brine and air temperatures leaving the evaporator and condenser, respectively. Since the loads are calculated using the heat balance on the refrigerant side, some modifications where brought to the original routine. The loads on the evaporator and condenser become inputs, while the latent and sensible heat exchanges are calculated.

ICE-CONCRETE SLAB

The ice-concrete slab model is used to predict the brine temperature leaving the ice-concrete slab and returning to the evaporator of the refrigeration system (point 1 in Figure 1) in terms of the ice temperature and brine temperature leaving the evaporator #2 and entering the slab (point 4). Using measurements from the monitored ice rink, a polynomial-type correlation-based model is developed:

$$T_{brine,out,slab} = A \cdot T_{brine,in,slab} + B \cdot T_{ice} + C \cdot T_{ice}^{\ 2} + D \cdot T_{ice}^{\ 3} + E \quad (5)$$

where A,B,C,D and E are coefficients that are estimated from the measurements, by using multiple correlation techniques (Statgraphics 2006). Table 3 lists the corresponding regressions coefficients, standard errors, t-Statistics and P-Values.

Table 3: Estimates and statistical indices for the slab correlation-based model

Parameter	Estimate	Standard error	t-Statistic	P-Value
A	0.708352	0.00663615	106.741	0
B	-0.127861	0.0216395	-5.90868	0
C	0.166354	0.00583716	2.84991	0.0044
D	0.0048402	0.00068860	7.02899	0
E	-1.40321	0.121146	-11.5827	0

The standard errors are very small for all coefficients, hence the values given can be considered as accurate. Since all t-statistics are significantly greater or less than zero, the correlation between variables is statistically significant. Because all P-Values are less than 0.05, each term is statistically significant at 95.0% confidence level. Thus, all coefficients and related variables should be kept in the model.

CONTROLLER

The controller model is based on the analysis of three monitored variables: the power input to the chillers and pump, the brine temperature at the slab exit, and the ice temperature. Empirical relations are determined between the brine temperature at the slab exit and the number of compressors in operation. The controller model stores in memory the brine temperature of the last eight minutes before the current reading to determine the required number of compressors in operation at current time step. The fluctuations of the return brine temperature and the required change in the number of compressors are illustrated in Figure 3, as an example.

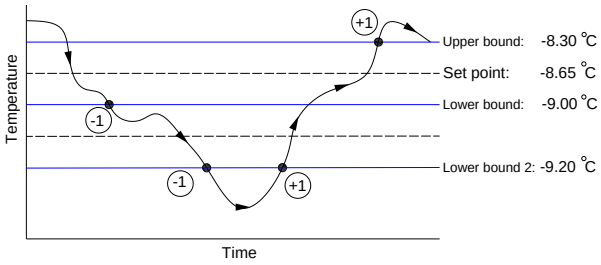

Figure 3: Variation of the brine temperature at the slab exit

Based on the analysis of measurements, a set point temperature of (-8.65°C) is defined. This temperature corresponds to the average brine temperature during one day. The controller does not instantly react when the brine temperature fluctuates around the set point. Hence, a dead band with an upper limit at (-8.30°C) and a lower limit at (-9.00°C) is defined. If the temperature is within the dead band, and tends to cross the upper or lower bound, one compressor is turned on (+1 in Figure 3) or off (-1), respectively. If the temperature is outside the dead band and crosses the boundaries towards the set point value, the number of compressors in operation is maintained constant. Further analysis allows defining a second temperature range, comprised between the lower bound of the dead band and a second lower bound defined at (-9.20°C). If the brine temperature crosses with a negative slope the second lower bound, one compressor is turned off (-1), while if it crosses with a positive slope, one compressor is turned on (+1). When the return brine temperature is maintained within the second temperature range, the number of compressors decreases every 10 minutes until a minimum of three compressors in operation is reached. However, if the return brine temperature is below the second lower bound, the number of compressors is decreased every 10 minutes until it reaches a minimum of two compressors. Regardless of the brine temperature fluctuations, if the number of compressors changes, the controller always wait 10 minutes before changing again the number of compressors in operation. For the start-up of the system, the controller turns on one compressor every 30 minutes until the return brine temperature reaches (-6°C). To avoid starting a compressor when the ice resurfacing occurs, the routine permanently verifies that the increase of the brine temperature is not caused by a sudden increase of the ice temperature. If the ice temperature reaches rapidly a temperature above (-6°C), the number of compressors in operation is maintained constant. Furthermore, a delay of 30 minutes is used between the decisions of the controller and the changes on the refrigeration system.

Low frequency noises of up to 0.1°C were noticed in the monitored temperatures at Camillien-Houde. Because the controller model is based on a set of rules depending on the return brine temperature, variations near the boundaries defined above may lead to instabilities in the controller operation, and therefore sudden changes in the number of compressors in operation. A second order low-pass filter is used to reduce those instabilities. The transfer function between the signal and the output in the Laplace space is given by (Antoniou 1979):

$$H(s) = \frac{{w_c}^2}{s^2 \cdot T^2 + 2 \cdot \xi \cdot w_c \cdot s + {w_c}^2} \qquad (6)$$

where $w_c = 2 \cdot \pi \cdot f_c$ (center frequency), f_c is the cut-off frequency, T is the period and ξ is the damping coefficient. Considering that the product of the damping coefficient (2ξ) is equal to $\sqrt{2}$, the transfer function of the signal in the Z space is given by the following relation:

$$\frac{O}{I} = \frac{a \cdot z + a}{b \cdot z - c} \qquad (7)$$

where $a = {w_c}^2 \cdot T^2$, $b = {w_c}^2 \cdot T^2 + 1.41 \cdot 2 \cdot w_c \cdot T + 4$ and $c = 4 + 1.41 \cdot 2 \cdot w_c \cdot T - {w_c}^2 \cdot T^2$. The rearrangement of equation 7 brings the following form relating the filtered output signal (O_t) in terms of the three constants (a, b, c), the past input at one time step prior to the current time I_{t-1} and filtered output O_{t-1}, and the actual input I_t:

$$O_t = \frac{[illegible] \cdot (I_t + I_{t-1}) + c \cdot O_{t-1}}{b} \qquad (8)$$

The period T is equal to the interval between measurements (60 seconds), while a center frequency at 0.016 Hz has been used leading to the following constants: a = 0.888, b = 7.546 and c = 5.769.

SIMULATION

The modular structure of TRNSYS 16 is the key point of its flexibility. The dynamic link library (DLL) structure allows users to integrate new component to the existing library by using any common programming languages (e.g., C, C++. Fortran). TRNSYS facilitates the integration of new components by generating a Fortran or a C++ template and a compiler project. The TRNSYS project includes all the settings required to generate a DLL. Therefore a C++ platform was created for the chiller, the ice-concrete slab and the controller models. Then, the code developed for each component

was integrated into the C++ platform, the files were compiled and the DLL exported and integrated into TRNSYS.

The simulation of the refrigeration system is based on the measurements collected during one day at one minute interval. The total power input (compressors, condensers and pump) is calculated and compared with measurements. The ice temperature, the refrigerant and brine mass flow rates, and the exterior air temperature are inputs to the model. Figure 4 presents the TRNSYS simulation flowchart:

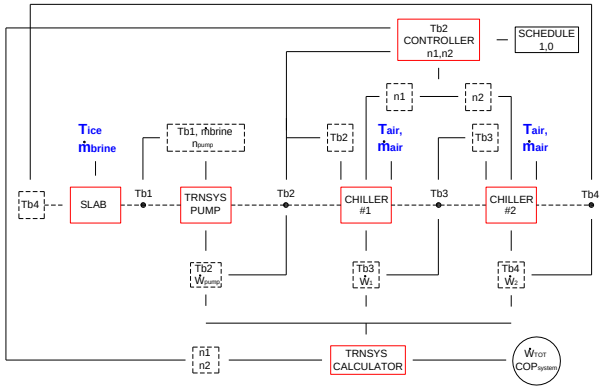

Figure 4: TRNSYS simulation flowchart

RESULTS

In order to evaluate the quality of results from the refrigeration system model, two types of simulation are performed: the open system and the closed system. The open system simulation consists of simulating the refrigeration system composed only of the correlation-based slab model, pump, and chillers, and leaving open the brine connection between the exit of chiller #2 and the inlet of the slab. The measured ice temperature and brine temperature entering the slab are used as inputs. The resulting brine temperature is compared with collected data at the exit of each component. A schedule is input, instead of a controller, to reproduce the exact variation of refrigeration load provided by the chiller, regardless of the brine temperature variation. Therefore, when comparing the calculated brine temperature at the exit of each component against the measured data, both are at the same refrigeration load and differences are only due to the component model.

Once the validity of each component is verified in an open-system simulation, the closed system is simulated. Connecting the brine temperature leaving the chiller #2 to the brine temperature entering the slab closes the refrigeration loop. For the closed loop simulation, the ice temperature is supplied to the refrigeration system model from an external file based on measurements made with an infrared camera above the blue line of the ice rink. Simulations are performed under two scenarios. First, the closed system simulation is performed employing a schedule of operation to test the stability of the numerical system. The temperature difference between measured and simulated results can lead to numerical instability that can be more easily identified if a common schedule is used instead of a controller. In the second scenario, the controller model is used instead of the given schedule of operation. This type of configuration allows for the evaluation of the auto-regulation of the refrigeration system when the only input supplied to the model is the ice temperature. The limits of the controller can then be tested. Next section presents the results for March 16th, 2006.

OPEN SYSTEM SIMULATION

Figures 5 and 6 present the measured and simulated brine temperatures at the exit of chiller #1 and #2, respectively, along with the number of compressors in operation.

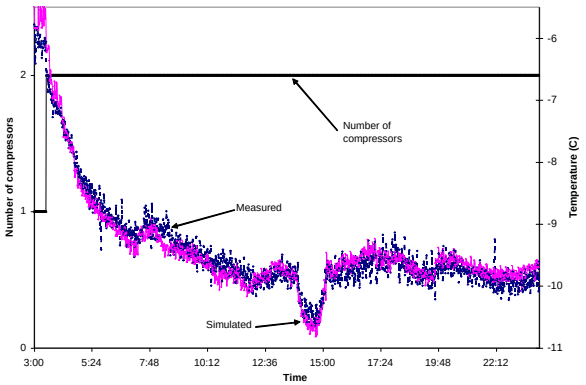

Figure 5: Open system simulation with given schedule. Measured vs simulated brine temperatures leaving chiller #1, and number of compressors in operation

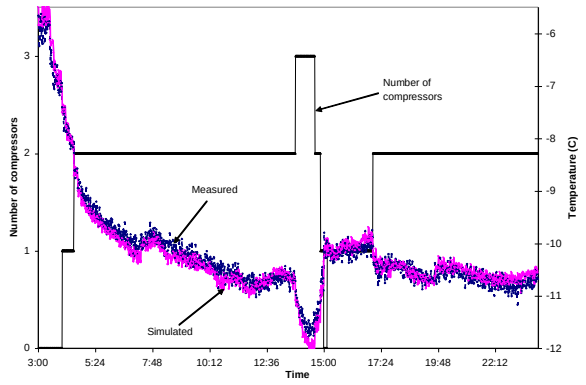

Figure 6: Open system simulation with given schedule. Measured vs simulated brine temperatures leaving chiller #2, and number of compressors in operation

The average error is of 0.16ºC (Figure 5) and 0.15ºC (Figure 6) that demonstrates a good agreement.

The data acquisition system installed in the ice rink records the total power input to compressors, pump and fans of air-cooled condensers. The total simulated power input simulated takes into account the compressor power input calculated by the chiller model, the pump power input by the TRNSYS pump model, and the approximated power input of 7 kW for each condenser when the compressor is in operation. Figure 7 shows the comparison between the measured and simulated total power input.

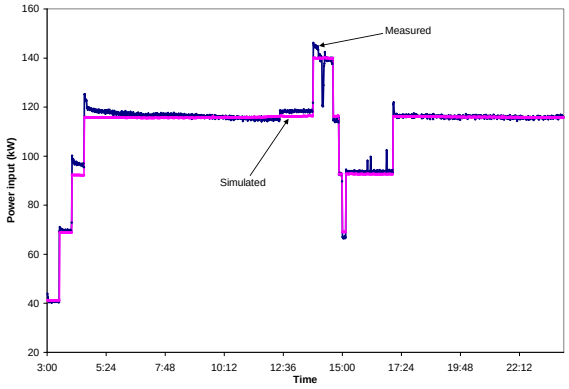

Figure 7: Open system simulation with given schedule. Measured vs simulated total power input

For the entire day, the simulated electricity use of the refrigeration system is 2,322 kWh/day while the measured electricity use is 2,338 kWh/day. The difference between the simulated and measured energy use is 16.1 kWh/day (0.69%), showing an excellent agreement.

CLOSED SYSTEM SIMULATION

Figure 8 presents the simulated brine temperature leaving the slab and the measured temperature as well as the total number of compressors in operation, as input by the given schedule. The average temperature difference is 0.35ºC, while in the open system it is of 0.15ºC. The difference is negligible.

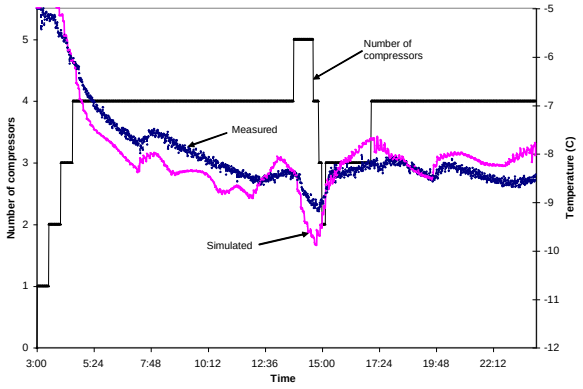

Figure 8: Closed system simulation with given schedule. Measured vs simulated brine temperature leaving the slab, and total number of compressors in operation

Figure 9 compares the simulated and measured brine temperature leaving the chiller #1. The average temperature difference is of 0.34ºC, while it is 0.16ºC in the open system configuration. The difference is also negligible.

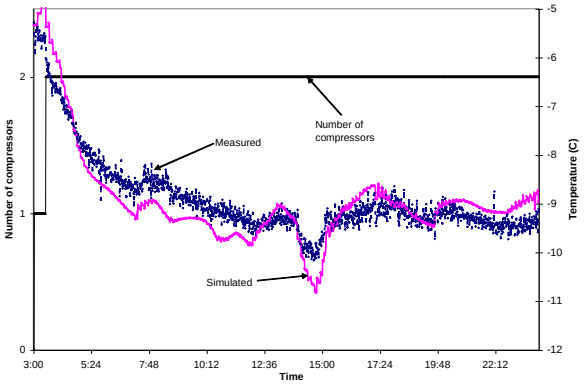

Figure 9: Closed system simulation with given schedule. Measured vs simulated brine temperature leaving chiller #1, and number of compressors in operation

Figure 10 compares the simulated and measured brine temperature leaving chiller #2. The number of compressors in operation in chiller #2 is also presented.

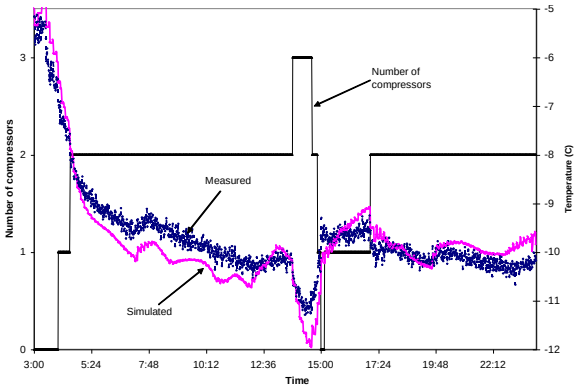

Figure 10: Closed system simulation with given schedule. Measured vs simulated brine temperatures leaving chiller #2, and number of compressors in operation

By comparing the brine temperature exiting chiller #1 (Figure 9) with that exiting chiller #2 (Figure 10), it can be observed that the shape of the curves is quite different. This difference is particularly evident in the interval between 13:45 and 15:00 when the number of compressors in chiller #2 changes several times. This result is coherent, because by switching on or off compressors in chiller #2, it decreases or increases the brine temperature. The average error at the exit of chiller #2 is of 0.33ºC in the closed configuration, while in open system configuration it is 0.15ºC.

Figure 11 presents the number of compressors in operation, based on measurements versus the simulated number using the controller model. The resulting number of compressors determined by the controller approximately fits the actual number. This shows that the controller is able to provide good result even if the brine temperature fluctuates (Figure 10).

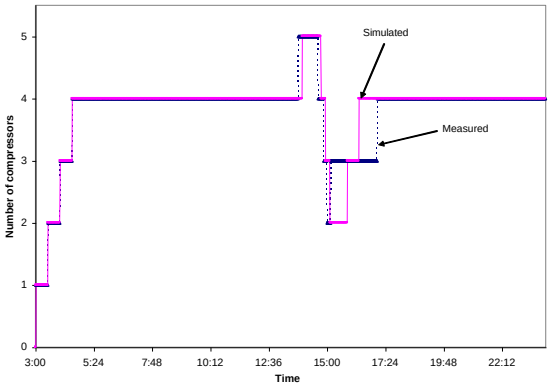

Figure 11: Closed system simulation with controller. Measured vs simulated number of compressors

Figure 12 compares the simulated and measured total power input to the refrigeration system in a closed loop configuration.

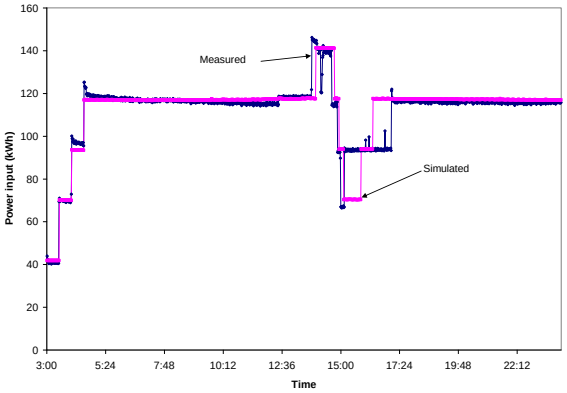

Figure 12: Closed system simulation with controller. Measured vs simulated total power input

The total simulated energy used by the refrigeration system is 2353 kWh/day while the measured electricity use is 2338 kWh/day. The difference is 15.37 kWh/day or 0.60%. This difference shows a good agreement between simulation and measurements.

HEAT RECOVERY FROM CONDENSERS

As an example of application, the computer model is used to estimate the energy savings when the heat rejected by the condensers is recovered and used for other heating needs. In this study, energy from the condensers is recovered to preheat the domestic hot water. Figure 13 presents the heat recovery system:

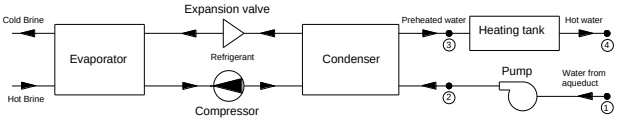

Figure 13: Heat recovery system

The water from the aqueduct (point 1) is pumped to the condenser where it is preheated (point 3). Then the water is stored in a tank where it reaches 60ºC (point 4) by using an additional energy source. The water supplied by the city's aqueduct has a variable temperature depending on the time of the year.

To evaluate the potential energy savings, it is necessary to determine the contribution of the condenser in the preheating process. Because the temperature of the sanitary water leaving the condenser (point 3) is not known, a sensitivity analysis is conducted to determine the heat recovered in terms of different water temperatures at the condenser exit. The refrigerant temperature limits the water temperature at point 3. Table 4 presents the potential energy recovered at different water temperatures, and the additional energy to be supplied to the heating tank to reach the set point temperature.

Table 4: Sensitivity analysis

Energy (kWh)	Water temperature at point 3		
	20ºC	30ºC	40ºC
Recovered	66.60	140.61	214.61
Supplied	296.01	222.01	148.01

The potential reduction of equivalent CO_2 emissions is calculated by using the total equivalent warming impact (TEWI) criterion, because it considers both the direct and indirect impacts of the refrigeration system over the lifetime of the system. Therefore, TEWI is used to evaluate the total emissions form the refrigeration and sanitary hot water systems.

The reference case corresponds to the actual ice rink, where the energy at the condenser is rejected to the outside air and the domestic hot water is heated using electricity. The corresponding emissions during 25 years are estimated at 7028 tons of CO_2. Table 4 presents the equivalent CO_2 emissions if the heat recovery system is used to preheat the hot water over the lifetime of the system (25 years).

Table 4: Equivalent CO_2 emissions, in tons, due to the heating of domestic hot water

	Water temperature at point 3		
	20ºC	30ºC	40ºC
CO_2 emissions	6882.6	6721.4	6560.3

If the temperature of the preheated water reaches 20ºC, the reduction of emissions would only be of 145.5 tons. However, if the temperature of the water at the condenser exit reaches 40ºC, the reductions of emissions would be of 267.7 tons, which is equivalent to about one year of operation of the ice rink.

CONCLUSIONS

A refrigeration system model of an existing ice rink, using a component approach, is presented in this study. The main three components are the following: chillers, ice-concrete slab and controller. Simulations have been performed using both open and closed loop systems. Good agreement is observed in both cases between simulation results and measurements.

ACKNOWLEDGEMENTS

The authors acknowledge the financial support from the National Sciences and Engineering Research Council of Canada (NSERC) as part of the strategic project STPGP 306792 (Development of conception tools and operating rules for the heating, ventilating, air conditioning and refrigeration systems of ice and curling rinks).

REFERENCES

Antoniou A. (1979), Digital Filters: *Analysis and Design*, McGraw-Hill Book Company.

ASHRAE (1998), *ASHRAE Handbook*, Atlanta: American Society of Heating, Refrigerating and Air-Conditioning Engineers, Inc.

Bourdouxhe J.P., Grodent M., and Lebrun J.J. (1994), 'HVAC1 Toolkit : Algorithms and Subroutines for Primary HVAC System Energy Calculations', ASHRAE.

Bellache O., Ouzzane M., and Galanis N. (2005a) 'Coupled condiction, convection, radiation heat transfer with simultaneous mass transfer in ice rinks', *Numerical Heat Transfer* 48(a) 219-238.

Bellache O., Ouzzane M., and Galanis N. (2005b) 'Numerical prediction of ventilation and thermal processes in ice rinks', *Building and Environment* 40(3) 417-426.

Daoud A., Galanis N. (2006) 'Calculation of the thermal loads of an ice rink using a zonal model and building energy simulation software', ASHRAE Transactions, 112 (2), pp. 526-537.

Gregoire G.B., Zilberberg Y.M. (1986) 'Computer aided thermal analysis of heat flow within the floor of an ice skating rink', Springer-Verlag, 263-285.

Jung M., Krarti M. (2007) 'Experimental analysis of heat transfer from ice rink floors', *Proceedings of the ASME International Solar Energy Conference, ISEC2006*, 681-687.

Ouzanne M., Zmeureanu R., Scott J., Sunyé R., Giguère D. (2006), 'Cooling load and environmental measurements in a Canadian indoor ice rink', ASHRAE Transactions, 112 (2) 538-545.

Scott J. 2003, 'Ultrasonic Chiller Validation: Liquid flow vs. Refrigerant Flow', Seminar 19, ASHRAE Winter Meeting, Chicago.

Statgraphics (2006), Statgraphics program, Centurion XV Version 14.2.00, StatPoint Ice.

Zmeureanu R., Zelaya E.M., Giguere, D. (2002) 'Simulation de la consommation d'énergie d'un aréna à l'aide du logiciel DOE-2.1E', eSim 2002 Conference, Montreal.